

# Machine Learning Algorithms Applied to the Identification of CPB06 Yield Criterion Parameters

Armando Marques<sup>1,5,a\*</sup>, Tomás Parreira<sup>1,5,b</sup>, Bernardete Ribeiro<sup>2,c</sup>,  
Pedro Prates<sup>1,3,4,5,d</sup>, André Pereira<sup>1,5,e</sup>

<sup>1</sup>CEMPRE, Department of Mechanical Engineering, University of Coimbra, Coimbra, Portugal

<sup>2</sup>CISUC, Department of Informatics Engineering, University of Coimbra, Coimbra, Portugal

<sup>3</sup>TEMA, Centre for Mechanical Technology and Automation, Department of Mechanical Engineering, University of Aveiro, Aveiro, Portugal

<sup>4</sup>LASI, Intelligent Systems Associate Laboratory, Guimarães, Portugal

<sup>5</sup>ARISE, Advanced Production and Intelligent Systems Associated Laboratory, Porto, Portugal

<sup>a\*</sup>armando.marques@uc.pt, <sup>b</sup>tomas.parreira@dem.uc.pt, <sup>c</sup>bribeiro@dei.uc.pt, <sup>d</sup>prates@ua.pt,  
<sup>e</sup>andre.pereira@uc.pt

\*corresponding author

**Keywords:** machine learning, constitutive modelling, parameter identification.

**Abstract.** In this work, a new methodology for the identification of the CPB06 yield criterion parameters is presented. This methodology is based on the application of Machine Learning models and the Levenberg-Marquardt optimization algorithm. The proposed methodology relies on data obtained from a biaxial tensile test with a cruciform specimen and aims to overcome some of the challenges usually faced during material characterization with the CPB06 yield criterion. The predictive performances achieved were positive overall, when comparing the yield surfaces obtained for testing cases, highlighting the potential of the proposed methodology.

## Introduction

Sheet metal forming is a manufacturing process of significant relevance for very competitive industries, such as the automotive and aerospace industries, due to its capability to produce high quantities of components at a relatively low cost [1]. Industrial demands dictate the need for constant innovation, in order to guarantee that quality, safety and environmental requirements are met while maintaining profits. In this context, Finite Element Analysis (FEA) is frequently used during process design and optimization, which requires an accurate representation of the material's mechanical behaviour. This representation is usually based on constitutive models [2].

Constitutive models typically have multiple material parameters which are determined from the response of the material during mechanical tests. As constitutive models become more flexible, the number of material parameters increases, which makes the parameter identification process more complex. In this context, researchers are looking for more efficient parameter identification strategies, with a recent focus on the application of Machine Learning (ML) algorithms to the solution of this problem. For example, Guo et al. [3] applied a deep learning model containing a convolutional neural network tasked with filtering noise from the available input data, and a long-short term neural network which makes the final predictions. After comparing the results obtained by the model with those obtained from an inverse method, in this case Finite Element Model Updating [4], the authors highlighted one of the main advantages of machine learning based methods, which is the prediction efficiency after the initial model is trained. Morand et al. [5] identified the parameters of a hardening law with non-unique solutions by applying a mixture of experts, which contained multiple neural networks. Since the hardening law considered can have multiple sets of parameters that represent the same hardening behaviour, the authors defended that a single model is incapable of obtaining good predictive performances, since it tends to average the parameter sets. As such, an ensemble model should be used.

The application of ML algorithms to the identification of more complex constitutive models presents its own challenges, partially because of the increasing number of parameters to identify, but also due to the characteristics of certain constitutive models, such as the fact that the CPB06 yield criterion [6] contains both discrete and continuous parameters. The presence of discrete parameters in particular is a limiting factor to the application of the typically used regression ML algorithms [7]. In this context, the main goal of this work is the development of an efficient identification strategy for the CPB06 yield criterion parameters, based on the application of ML algorithms, and the Levenberg-Marquardt optimization algorithm, considering a dataset that contains the results of a single biaxial tensile test on a cruciform sample.

## Procedure

### Numerical Models.

In this work, the mechanical response of the materials was evaluated from the numerical results obtained from a biaxial tensile test on a cruciform sample. Fig. 1 a) presents the geometry of the cruciform sample, originally proposed in [8]. Each arm has a total length of 73.6 mm and the initial thickness is 0.5 mm. The specimen was discretized with a finite element mesh, as shown in Fig. 1 b), which contains 6680 eight-node hexagonal solid elements. Only one eighth of the specimen is modelled, due to material and geometrical symmetries. During the simulation, a prescribed displacement of 2 mm was imposed in the grip region of both arms, simultaneously, along the x and y directions. The in-house finite element code DD3IMP, developed and optimized for the simulation of metal forming processes, was used to carry out the simulation in this work [9–11].

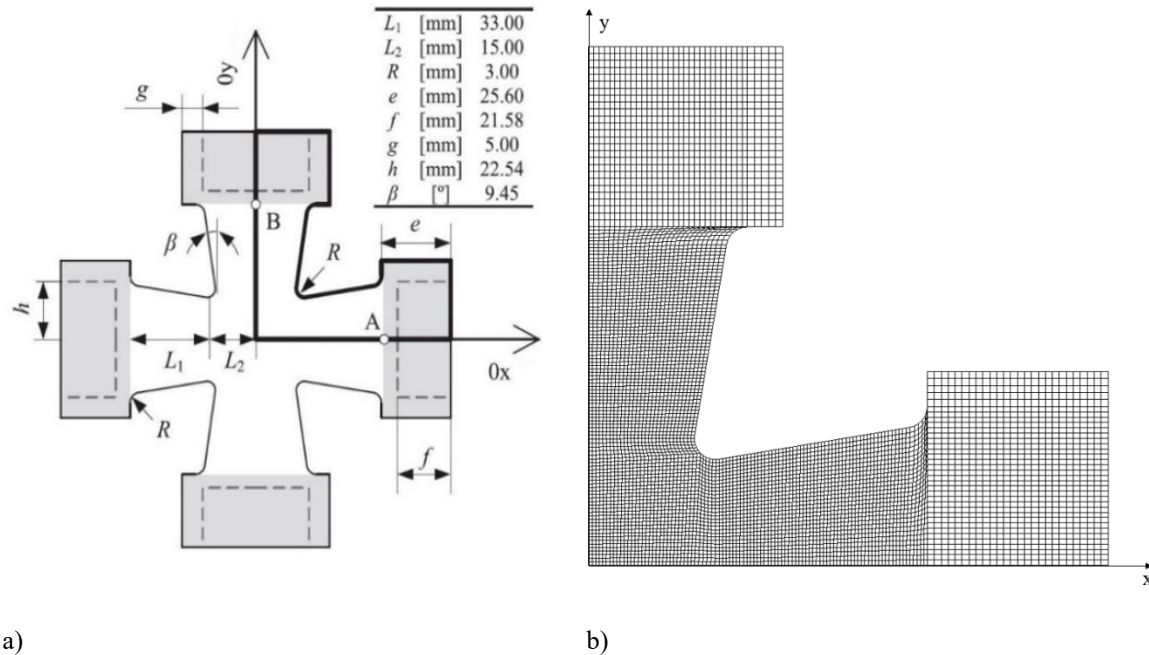


**Fig. 1.** a) Geometry of the cruciform specimen [8]; b) Finite element mesh used to discretize one eighth of the specimen.

The constitutive model used for this work assumes an isotropic elastic behaviour, described by the generalized Hooke's law, and an anisotropic plastic behaviour, described by the orthotropic CPB06 yield criterion [6] and the Swift hardening law [12].

The CPB06 orthotropic yield criterion is based on the isotropic yield criterion given by:

$$[ (|s_1| - ks_1)^a + (|s_2| - ks_2)^a + (|s_3| - ks_3)^a ]^{\frac{1}{a}} = Y, \quad (1)$$

where  $s_1$ ,  $s_2$  and  $s_3$  are the principal values of  $\mathbf{s} = \boldsymbol{\sigma}'$ ,  $\boldsymbol{\sigma}'$  is the deviatoric stress tensor and  $Y$  is the yield stress and its evolution during deformation. Parameter  $a$  is a positive integer, and  $k$  is a coefficient that represents the ratio between tensile and compression yield stresses, given by:

$$k = \frac{1-h}{1+h}, \text{ with } h = \left[ \frac{2^a - 2 \left( \frac{\sigma^T}{\sigma^C} \right)^a}{2 \left( \frac{\sigma^T}{\sigma^C} \right)^a - 2} \right]^{\frac{1}{a}}, \quad (2)$$

where  $\sigma^T$  and  $\sigma^C$  are the yield stresses in tension and compression, respectively. If  $k = 0$ , the responses in tension and compression are equal. For  $k = 0$  and  $a = 2$ , this criterion is equivalent to von Mises. Convexity is guaranteed for  $a \geq 1$  and  $k \in [-1, 1]$ . To extend this criterion to orthotropy, a linear transformation is applied to the deviatoric stress tensor. In this new criterion,  $s_1, s_2$  and  $s_3$  are the principal values of  $\mathbf{s} = \mathbf{C}\boldsymbol{\sigma}'$ , where  $\mathbf{C}$  is a constant fourth order tensor, containing 9 independent anisotropy coefficients, given by:

$$\mathbf{C} = \begin{bmatrix} C_{11} & C_{12} & C_{13} & 0 & 0 & 0 \\ C_{12} & C_{22} & C_{23} & 0 & 0 & 0 \\ C_{13} & C_{23} & C_{33} & 0 & 0 & 0 \\ 0 & 0 & 0 & C_{44} & 0 & 0 \\ 0 & 0 & 0 & 0 & C_{55} & 0 \\ 0 & 0 & 0 & 0 & 0 & C_{66} \end{bmatrix}. \quad (3)$$

This criterion can be written in the form:

$$B[(|s_1| - ks_1)^a + (|s_2| - ks_2)^a + (|s_3| - ks_3)^a]^{\frac{1}{a}} = Y, \quad (4)$$

where  $B$  is a constant that guarantees that the yield stress  $Y$  is identical to the tensile yield stress in the rolling direction. given by:

$$B = \left[ \frac{1}{(|\phi_1| - k\phi_1)^a + (|\phi_2| - k\phi_2)^a + (|\phi_3| - k\phi_3)^a} \right]^{\frac{1}{a}}, \quad (5)$$

with

$$\phi_1 = (2/3)C_{11} - (1/3)C_{12} - (1/3)C_{13}, \quad (6)$$

$$\phi_2 = (2/3)C_{21} - (1/3)C_{22} - (1/3)C_{23}, \quad (7)$$

$$\phi_3 = (2/3)C_{31} - (1/3)C_{32} - (1/3)C_{33}. \quad (8)$$

This criterion can be reduced to von Mises, for  $k = 0$ ,  $a = 2$  and  $\mathbf{C}$  equal to the 4<sup>th</sup> order identity tensor. When applied to metallic sheets, the condition  $C_{44} = C_{55} = 1$  as in isotropy is assumed. Also,  $C_{11}$  is usually considered equal to 1, ensuring that all sets of parameters are unique.

The Swift hardening law is given by the following equation:

$$Y = K (\varepsilon_0 + \bar{\varepsilon}^p)^n \quad (9)$$

where  $\bar{\varepsilon}^p$  is the equivalent plastic strain and  $K$ ,  $\varepsilon_0$  and  $n$  are material parameters. The initial yield stress,  $Y_0$ , is given by:

$$Y_0 = K \varepsilon_0^n \quad (10)$$

### Dataset Generation.

The dataset used in this work contains the numerical results of the biaxial tensile tests as input data. This data includes force measurements along the  $\theta_x$  and  $\theta_y$  axis, as well as the  $\varepsilon_{xx}$ ,  $\varepsilon_{yy}$  and  $\varepsilon_{xy}$  components of the strain tensor. The forces were measured for displacement increments of 0.4 mm, up to a total displacement of 2 mm, considering that this displacement increment is the same along both axes. The strain measurements were obtained from the final instant of the mechanical test, which corresponds to a displacement of 2 mm. In order to improve efficiency, the dataset size was limited,

by considering only the strain measurements that are most sensitive to the variation of the constitutive model, this sensitivity was evaluated by comparing the standard deviation of the strain values across the entries in the dataset. In total, 15 strain measurements were considered, which were obtained from 10 different points in the specimen. Fig 2 shows the distribution of the Cauchy stress tensor components  $\sigma_{xx}$ ,  $\sigma_{yy}$  and  $\sigma_{xy}$  on the cruciform specimen, obtained for the isotropic case. It can be observed that shear and biaxial stress data can be obtained in the notched region of the specimen, while the arms provide uniaxial stress data. As such, it is expected that the information obtained from this mechanical test will allow for a proper identification of the yield criterion parameters.

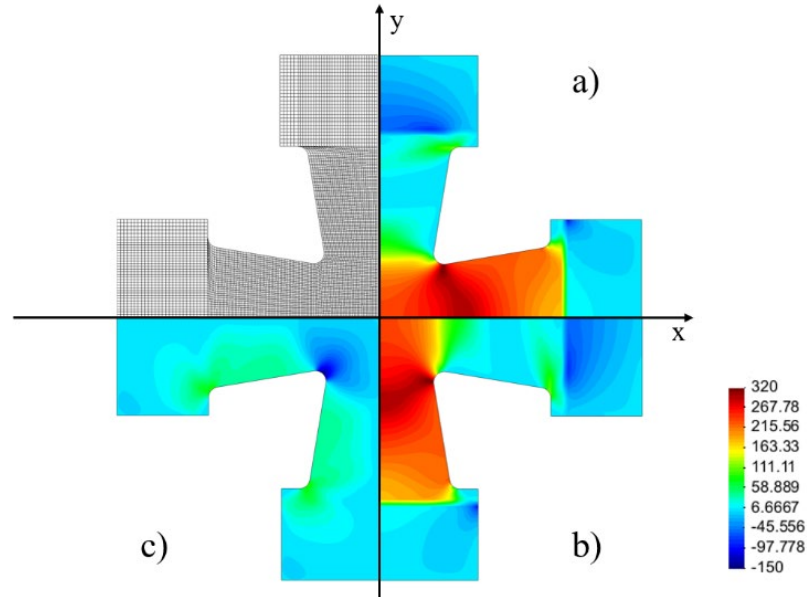


**Fig. 2.** Stress fields obtained for a biaxial tensile test for a total displacement of 2mm, a)  $\sigma_{xx}$ , b)  $\sigma_{yy}$ , c)  $\sigma_{xy}$ .

In order to be able to identify the constitutive model parameters independently of the elastic behaviour of the material, the Young's Modulus is also considered as an input ( $E$ ). The output data consists of the parameters to be identified, namely the  $C_{22}$ ,  $C_{33}$ ,  $C_{66}$ ,  $C_{12}$ ,  $C_{13}$ ,  $C_{23}$  (collectively referred to as  $C_{ij}$  from now on) and  $\alpha$  parameters of the CPB06 yield criterion. The limits of the  $C_{ij}$  parameters are presented in Table 1, which correspond to a deviation of  $\pm 1.5$  relatively to the isotropic values. For the  $\alpha$  parameter, which is a positive integer, the values of 2 and 4 were considered. Since the mechanical test considered does not contain compression data, tension compression symmetry will be considered, and as such,  $k = 0$  was assumed for all materials. Also, 3 different values of  $E$  were considered, 70, 140 and 210 GPa, which are typical values for Aluminium, Titanium and Steel alloys, respectively.

**Table 1.** Limits of each parameter used to generate the material constitutive model parameter sets.

	$C_{22}$	$C_{33}$	$C_{66}$	$C_{12}$	$C_{13}$	$C_{23}$
Lower Limit	-0.5	-0.5	-0.5	-1.5	-1.5	-1.5
Upper Limit	2.5	2.5	2.5	1.5	1.5	1.5

The dataset can be divided into a training set and a testing set. The training set is used during the training process by the algorithms, while the testing set is used to evaluate the predictive performance of the trained models. The training set contains 4500 different sets of constitutive parameters for each value of  $\alpha$ , while the testing set contains 500 sets of parameters for each value of  $\alpha$ . These parameter sets were generated by a Sobol sequence, which provides a more uniform parameter distribution than a purely random distribution. After the parameter sets were established, each material was assigned a value of  $E$ , in a uniform distribution.

### Machine Learning.

Machine learning (ML) is a field of study focused on the development of systems capable of improving themselves without explicit programming [13]. ML algorithms are frequently applied to the solution of complex problems which would otherwise require building first-principle models which can be prohibitively expensive and time-consuming. The ML algorithm used in this work is the Multi-Layer Perceptron (MLP), a supervised algorithm [14]. Supervised algorithms learn from labelled data, through a process typically called training. This process consists of mapping the relations between input and output variables in the training data. During the training process, model internal parameters are calibrated, allowing it to predict outputs for new sets of inputs.

The MLP is a feed forward neural network, which can be applied to both classification and regression problems, and supports multi-output problems natively [15]. An MLP model is composed of multiple layers of nodes, in which each node connects to the nodes of the following layer, passing information. The first layer is called input layer and contains one node per input variable in the dataset. This layer is followed by any number of layers called hidden layers. The number of hidden layers, as well as the number of nodes in each of these layers are defined before the training process. The output of a single node from a hidden layer is given by:

$$z_i = \emptyset(\sum_j w_{ij}z'_j + d_i), \quad (11)$$

where  $z_i$  is the output of node  $i$  from the current layer,  $z'_j$  is the output of  $j$  from the previous layer,  $w_{ij}$  is the weight associated with  $z'_j$ ,  $d_i$  is a bias term and  $\emptyset$  is a non-linear activation function. The last layer, called the output layer, is responsible for making the final predictions, based on the information received from the previous layer. The training process of an MLP model is an iterative process based on the backpropagation algorithm [16]. For each iteration, the algorithm evaluates whether each of the model weights should be increased or decreased in order to increase predictive performance, and then all weights of the network are changed accordingly, by a small increment.

### Methodology

The proposed methodology for the identification of the CPB06 yield criterion parameters includes the application of both classification and regression MLP models, which were constructed with the publicly available python library Scikit-learn [17]. The first step in the methodology is the identification of the  $\alpha$  parameter. This step is accomplished by a classification model, which was trained with the mechanical test results (forces and strains) and the elastic parameter  $E$  as inputs. Then, the remaining parameters are identified. Due to the complexity of this identification, an iterative optimization process is adopted. First, a ML model is trained for each value of the parameter  $\alpha$  considered. These models use the constitutive model parameters as input and predict the results of the mechanical test considered in the dataset. Then, the results of this prediction are compared with the real results, and through the Levenberg-Marquardt algorithm, the  $C_{ij}$  parameters of the CPB06 yield criterion are optimized. A schematic representation of the proposed methodology is presented in Fig 3.

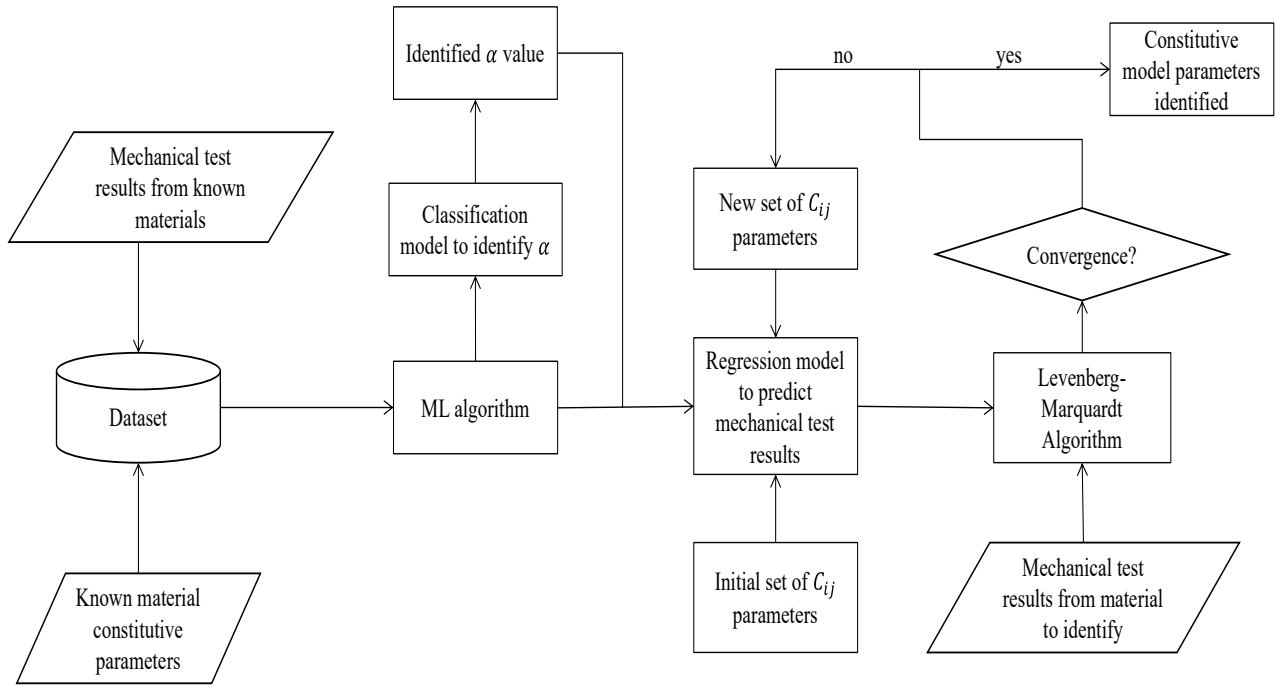


**Fig. 3.** Schematic representation of the proposed methodology.

During the optimization process, the value of the  $\alpha$  parameter considered is the one identified in the first step of the methodology. The objective function used in the optimization process is the weighted sum of squared residuals function, and finite differences are used to compute the Jacobian matrix, which is required for the application of the Levenberg-Marquardt algorithm.

### Model training.

The ML model for the first identification step was trained with a total of 4000 materials from the training set, 2000 corresponding to each value of the  $\alpha$  parameter. For the second identification step, 2 models were trained, one for each value of  $\alpha$ . Each of those models was trained with a total of 4500 materials. All data was scaled with z-score normalization [18]. Each model had its hyperparameters optimized before the training of the final models. In this work, this optimization process consists of a trial-and-error approach, in which the training set is divided, randomly into two temporary sets, one to train temporary models and another to validate the performance of these temporary models. The validation sets include 30% of the total training set data, and the random data split is repeated 10 times. The hyperparameters that led to the best average performance across the temporary models were chosen to train the final model, with all the training set data. These hyperparameters include the tanh activation function and the limited-memory BFGS (LBFGS) solver.

### Performance Evaluation.

The predictive performance of the ML models was evaluated with performance metrics. Two metrics were considered, accuracy and relative error (RE). Accuracy is given by the following equation:

$$\text{Accuracy} = (\text{Correct predictions})/(\text{All predictions}). \quad (12)$$

This metric represents the ratio of correct prediction made by a model and is used to evaluate the classification ML model used to identify the parameter  $\alpha$ . RE is given by:

$$\text{RE} = \frac{y_i - y_i^*}{y_i}, \quad (13)$$

where  $y$  and  $y^*$  are the real and predicted values for the variables in analysis, respectively. This metric is used to evaluate the performance of regression models.

## Results

In order to evaluate the predictive performance of the proposed methodology, the trained models were used to make predictions for the testing set, and the performance metrics were calculated. The ML model responsible for the first identification step, which is the identification of the  $\alpha$  parameter, achieved an accuracy of 83.55%. While this performance leaves room for improvement, it can be considered acceptable, especially considering that the impact of an incorrect prediction in this step can only be properly measured when the remaining CPB06 parameters are identified, and the resulting mechanical behaviours can be compared. This comparison, after the remaining CPB06 parameters are identified in the second identification step, is based on various results, including the values of yield stress for uniaxial tension ( $\sigma$ ), measured for angles of 15°, 30°, 45°, 60°, 75° and 90° in relation to the rolling direction, shear stress ( $\tau$ ), for angles of 0°, 15°, 30° and 45° in relation to the rolling direction, and the Lankford coefficients, or anisotropy coefficients ( $r$ ) for angles of 0°, 15°, 30°, 45°, 60°, 75° and 90° in relation to the rolling direction. Additionally, the values of  $\sigma_b$  and  $r_b$ , which are the yield stress under biaxial loading and biaxial anisotropic coefficient [19], are considered. It is preferable to compare these values, which partially describe the yield surface, instead of comparing the yield criterion parameters directly. This is because multiple combinations of parameters can lead to very similar yield surfaces, due to interactions between parameters.

The results obtained after the second identification step are shown in Fig. 4 and 5. These results are separated by the values of  $\alpha$  of the original materials in the testing set. However, it is worth mentioning that the value of  $\alpha$  considered in each prediction is the one obtained from the first identification step.

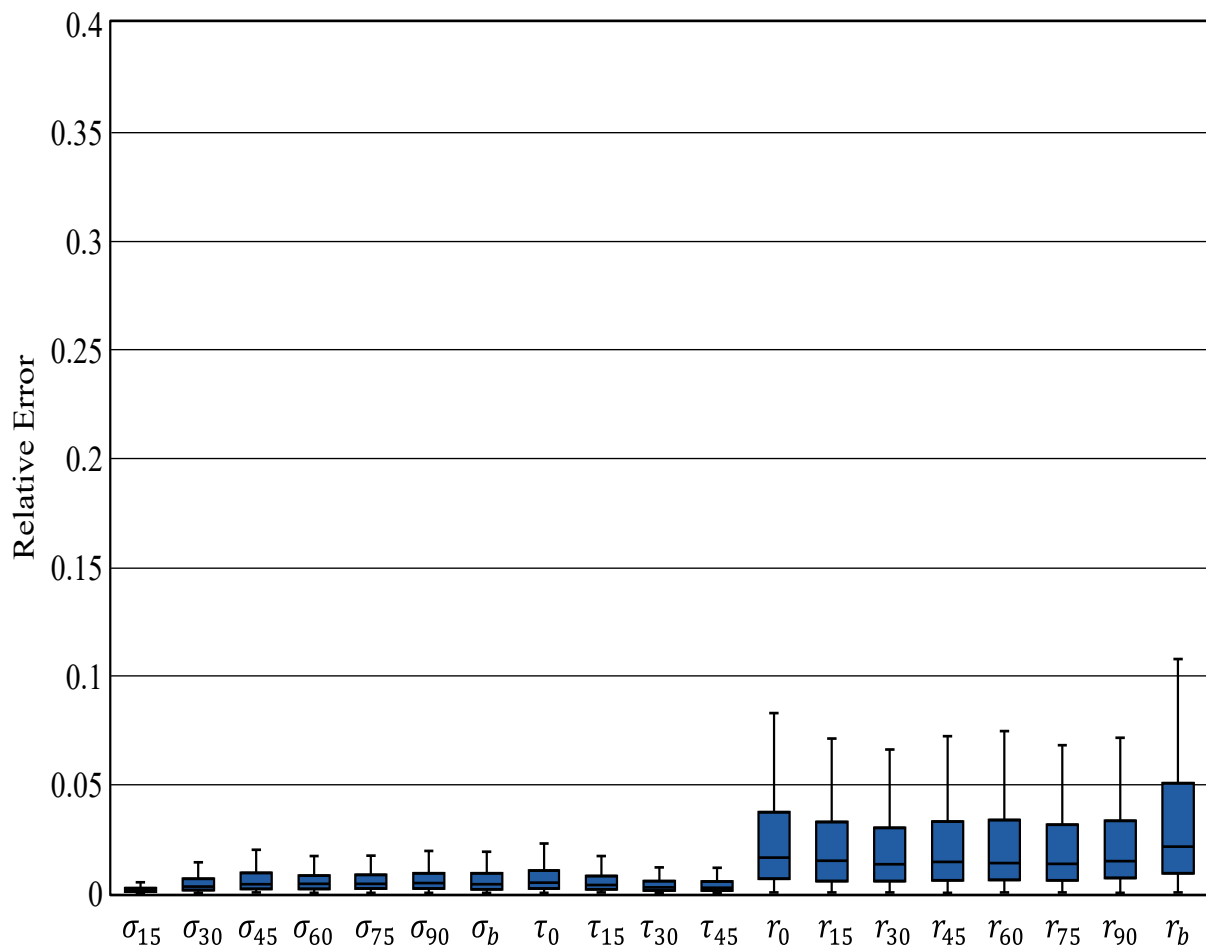


**Fig. 4.** Relative Error distribution obtained after the prediction of the CPB06 yield criterion parameters, for the materials with a real  $\alpha$  value of 2.

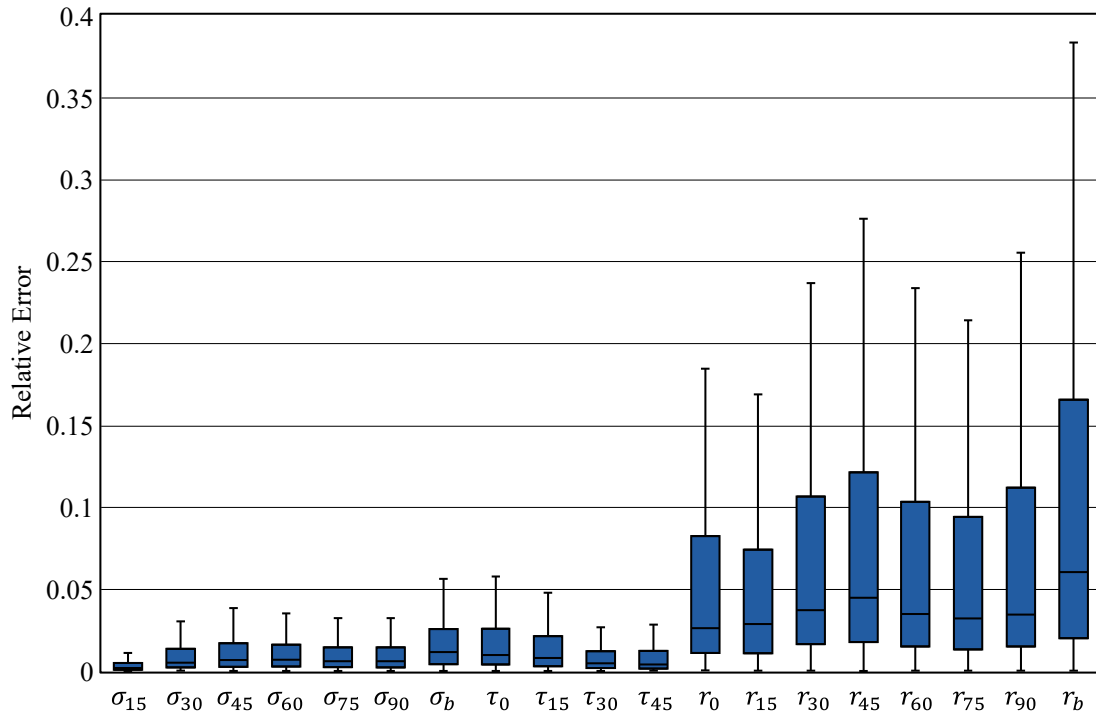


**Fig. 5.** Relative Error distribution obtained after the prediction of the CPB06 yield criterion parameters, for the materials with a real  $\alpha$  value of 4.

Overall, the predictive performances obtained are considered positive. The yield stresses in particular show a good agreement between the real yield surfaces and the yield surfaces that correspond to the identified parameters, with RE values that are frequently under 2%, and median RE values under 1%, for both values of  $\alpha$ . Regarding the anisotropy coefficients, except  $r_b$ , the RE values achieved are higher than the ones for the yield stresses, particularly for the  $\alpha$  value of 4, but they can still be considered positive, with median RE values under 5% for all cases. These positive results show that the incorrect identifications for the value of  $\alpha$ , during the first identification step, didn't significantly compromise the overall quality of the identification process. This means that during the optimization process, the proposed methodology could identify sets of CPB06 parameters that closely matched the mechanical behaviour of the real parameter sets.

The values of RE obtained for  $r_b$  are higher than those obtained for the remaining variables, particularly for the  $\alpha$  value of 4. This difference may be explained by the available input data. The input data considered may not accurately represent the biaxial stress state associated with this anisotropic coefficient. The inclusion of more input data, representative of other stress states, can help improve the proposed methodology, however, it is worth noting that this will likely require more mechanical tests to be performed, which will increase the cost of the identification process.

## Conclusion

In this work, a parameter identification methodology for the CPB06 yield criterion was proposed. This methodology pairs the use of regression and classification ML models, with the application of the Levenberg-Marquardt optimization algorithm. The dataset created for this purpose contains the results of a biaxial tensile test with a cruciform specimen, which was used to train and test the ML models and the general predictive performance of the methodology.

The results highlight the potential of the proposed methodology, with the predicted yield surfaces showing good agreement with the real ones from the testing set, especially when comparing yield stress values. Improvements to the current methodology are possible by including more data, which represents different stress-states.

The methodology presented leaves some questions to explore in future work. First, the methodology will be expanded for more values of  $\alpha$ . The exploration of alternative ML algorithms is

also of interest. In order to validate the methodology for an industrial environment, a more rigorous definition of the strain measurement points is necessary, and the robustness to the presence of noise in the data should also be explored. This can be achieved either with real experimental data, or with numerical data with artificial noise. Finally, the performance and efficiency of the methodology will be compared with other parameter identification methodologies.

### Acknowledgement

This research is sponsored by national funds through FCT – Fundação para a Ciência e a Tecnologia, under projects UID/00285/2025 (<https://doi.org/10.54499/UID/00285/2025>) and LA/P/0112/2020 (<https://doi.org/10.54499/LA/P/0112/2020>). It was also supported by the projects RealForm (ref. 2022.02370.PTDC), SmartBending (ref. 2023.14606.PEX), LSD-TRIP (ref. COMPETE2030-FEDER-00778700) and A3Shell (ref. COMPETE2030-FEDER-02233400). Tomás Parreira was supported by a grant for scientific research from FCT (ref. 2024.00961.BD). All support is gratefully acknowledged.

### References

- [1] Marques AE, Parreira TG, Pereira AFG, et al (2025) Machine learning application to the identification of sheet metal constitutive model parameters. *Machine Learning for Computational Science and Engineering* 1:. <https://doi.org/10.1007/s44379-024-00006-8>.
- [2] Yoshida F, Hamasaki H, Uemori T (2013) A user-friendly 3D yield function to describe anisotropy of steel sheets. *International Journal of Plasticity* 45:119–139. <https://doi.org/10.1016/j.ijplas.2013.01.010>.
- [3] Guo Z, Bai R, Lei Z, et al (2021) CPINet: Parameter identification of path-dependent constitutive model with automatic denoising based on CNN-LSTM. *European Journal of Mechanics, A/Solids* 90:104327. <https://doi.org/10.1016/j.euromechsol.2021.104327>.
- [4] Prates PA, Pereira AFG, Sakharova NA, et al (2016) Inverse Strategies for Identifying the Parameters of Constitutive Laws of Metal Sheets. *Advances in Materials Science and Engineering* 2016:. <https://doi.org/10.1155/2016/4152963>.
- [5] Morand L, Helm D (2019) A mixture of experts approach to handle ambiguities in parameter identification problems in material modeling. *Computational Materials Science* 167:85–91. <https://doi.org/10.1016/j.commatsci.2019.04.003>.
- [6] Cazacu O, Plunkett B, Barlat F (2006) Orthotropic yield criterion for hexagonal closed packed metals. *International Journal of Plasticity* 22:1171–1194. <https://doi.org/10.1016/j.ijplas.2005.06.001>.
- [7] Marques AE, Parreira TG, Pereira AFG, et al (2024) Machine learning applications in sheet metal constitutive Modelling : A review. *International Journal of Solids and Structures* 303:. <https://doi.org/10.1016/j.ijsolstr.2024.113024>.
- [8] Prates PA, Oliveira MC, Fernandes J V. (2014) A new strategy for the simultaneous identification of constitutive laws parameters of metal sheets using a single test. *Computational Materials Science* 85:102–120. <https://doi.org/10.1016/j.commatsci.2013.12.043>.
- [9] Menezes LF, Teodosiu C (2000) Three-dimensional numerical simulation of the deep-drawing process using solid finite elements. *Journal of Materials Processing Technology* 97:100–106. [https://doi.org/10.1016/S0924-0136\(99\)00345-3](https://doi.org/10.1016/S0924-0136(99)00345-3).
- [10] Oliveira MC, Alves JL, Menezes LF (2008) Algorithms and strategies for treatment of large deformation frictional contact in the numerical simulation of deep drawing process. *Archives of Computational Methods in Engineering* 15:113–162. <https://doi.org/10.1007/s11831-008-9018-x>.

- 
- [11] Neto DM, Oliveira MC, Menezes LF (2017) Surface Smoothing Procedures in Computational Contact Mechanics. *Archives of Computational Methods in Engineering* 24:37–87. <https://doi.org/10.1007/s11831-015-9159-7>.
- [12] Swift HW (1952) Plastic instability under plane stress. *Journal of the Mechanics and Physics of Solids* 1:1–18. [https://doi.org/10.1016/0022-5096\(52\)90002-1](https://doi.org/10.1016/0022-5096(52)90002-1).
- [13] Jang DP, Fazily P, Yoon JW (2021) Machine learning-based constitutive model for J2-plasticity. *International Journal of Plasticity* 138:102919. <https://doi.org/10.1016/j.ijplas.2020.102919>.
- [14] Zhou ZH (2018) A brief introduction to weakly supervised learning. *National Science Review* 5:44–53. <https://doi.org/10.1093/nsr/nwx106>.
- [15] Murtagh F (1991) Multilayer perceptrons for classification and regression. *Neurocomputing* 2:183–197. [https://doi.org/10.1016/0925-2312\(91\)90023-5](https://doi.org/10.1016/0925-2312(91)90023-5).
- [16] Dreyfus SE (1990) Artificial Neural Networks, Back Propagation, and the Kelley-Bryson Gradient Procedure. *Journal of Guidance, Control, and Dynamics* 13:926–928. <https://doi.org/10.2514/3.25422>.
- [17] Pedregosa F, Varoquaux G, Gramfort A, et al (2012) Scikit-learn: Machine Learning in Python. *Journal of Machine Learning Research* 12:2825–2830.
- [18] Pandey A, Jain A (2017) Comparative Analysis of KNN Algorithm using Various Normalization Techniques. *International Journal of Computer Network and Information Security* 9:36–42. <https://doi.org/10.5815/ijcnis.2017.11.04>.
- [19] Barlat F, Brem JC, Yoon JW, et al (2003) Plane stress yield function for aluminum alloy sheets - Part 1: Theory. *International Journal of Plasticity* 19:1297–1319. [https://doi.org/10.1016/S0749-6419\(02\)00019-0](https://doi.org/10.1016/S0749-6419(02)00019-0).